Available on CMS information server **CMS IN 2003-030**

CMS Internal Note

The content of this note is intended for CMS internal use and distribution only

5 August 2003

Performance of the CMS tracker analog optical link lasers exposed to high magnetic fields

Th.Bauer, M.Friedl

Institute of High Energy Physics, Vienna, Austria

Abstract

The CMS Silicon Strip Tracker will be equipped with 36392 analog optical links. These links include edge-emitting InGaAsP multi-quantum-well (MQW) lasers operating at $1310\,\mathrm{nm}$ which will be located within the tracker volume at an ambient temperature of -10° C and a magnetic field of $4\,\mathrm{T}$. To confirm the suitability of final candidate lasers for operation in the $4\,\mathrm{T}$ field, four devices were exposed to magnetic field strengths up to $10\,\mathrm{T}$ in all three geometrical orientations. The influence of the field to the optical spectrum and the transfer characteristics was measured. Moreover, an APV25 readout chip was tested inside the magnetic field. All tested devices showed no significant performance degradation within the accuracy of the measurements.

1 Introduction

A schematics of the CMS tracker readout chain is illustrated in fig. 1. The silicon strip detectors of the experiment will be read out by 72784 APV25 readout-chips [1]. The outputs of groups of two chips will be multiplexed onto a single line, which is then transfered via an analog optical link to the Frontend Driver (FED). Edge-emitting InGaAsP multi-quantum-well semiconductor lasers emitting at a wavelength of $1310\,\mathrm{nm}$ were chosen for the application in the CMS optical links [2, 3]. These transmitters will be exposed to heavy radiation and very high magnetic fields up to $4\,\mathrm{T}$ during operation in the CMS tracker.

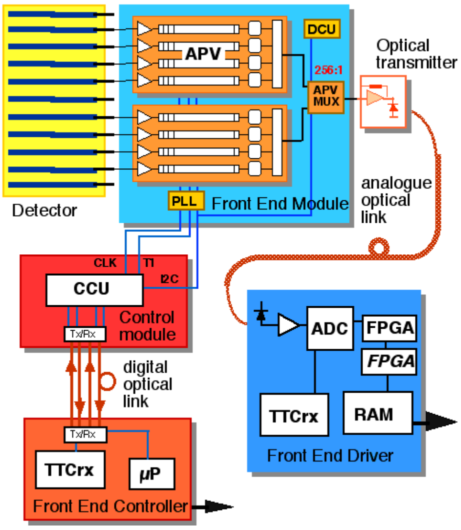

Figure 1: Tracker readout and control schematics

The effect of magnetic fields up to $2.4\,\mathrm{T}$ on the performance of the lasers has already been investigated by the collaboration [4]. The aim of the present test was to reach the expected field strength of $4\,\mathrm{T}$ and to exceed it up to $10\,\mathrm{T}$ in order to investigate, with a generous safety margin, if any performance degradation of the lasers and the APV25 readout chip can be observed.

2 Characteristics of multi-quantum-well lasers

2.1 Optical performance

A sample spectrum of a multi-quantum-well (MQW) laser consisting of several Fabry Perot modes around a center wavelength is shown in fig. 2. These spectral characteristics vary according to change of temperature and bias current.

When the temperature is raised, the bandgap energy is lowered down causing a red shift of the peak wavelength. When the temperature is raised, the spectral peaks are expected to red-shift at a rate of $0.1\,\mathrm{nm/K}$ for the devices used in this study. [5]

The effect of a wavelength shift caused by a strong magnetic field has already been investigated for various types of semiconductor lasers at different temperatures [7, 8, 9]. The wavelength shift found by these experiments is in general very small and of the order of $\ll 0.1\,\mathrm{nm/T}$. A measurement done by the CMS collaboration for fields up to $2.4\mathrm{T}$ showed no effect within the accuracy of the measurement [4]. Results obtained as part of this study are shown in section 4.

2.2 Analog performance

A sample transfer function of a tested laser is shown in (fig. 3). It can be seen that the device only lases if the driving current exceeds a threshold current. Both, the threshold current and the laser efficiency are very sensitive to temperature. The threshold current typically increases by the order of $0.1\,\mathrm{mA/K}$ at room temperature [10], while slope efficiency usually decreases above room temperature.

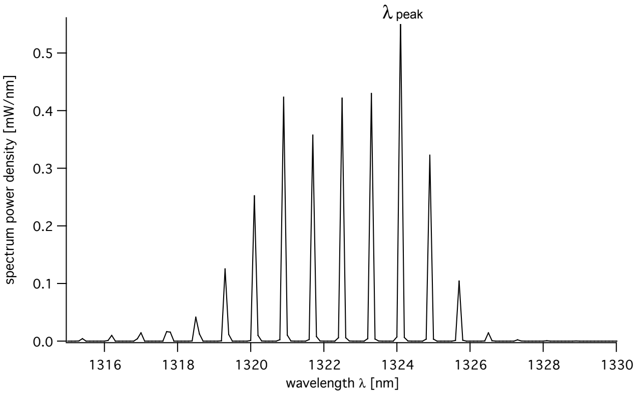

Figure 2: spectrum of a InGaAsP MQW laser

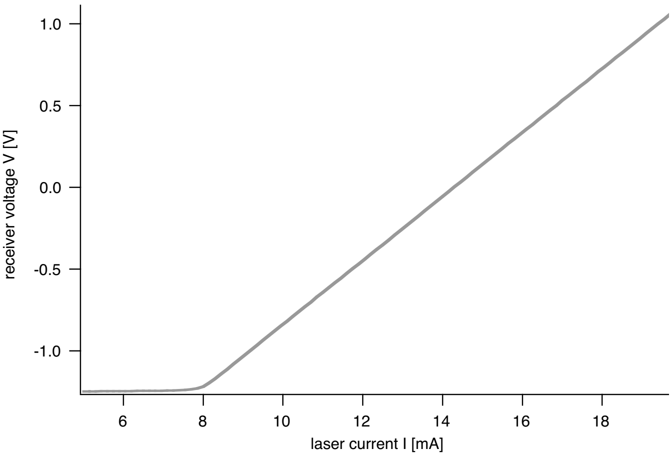

Figure 3: transfer function of a InGaAsP MQW laser

Threshold current shifts caused by high magetic fields for different types of semiconductor lasers have been reported by several authors [7] [11]. No threshold current shifts have been observed to present devices and fields up to $2.4\mathrm{T}$ by the collaboration [4]. This indicates the effect to be smaller than $0.05\,\mathrm{mA/K}$. Measurable threshold current shifts could possibly be observed at higher operating currents and field strengths. The collaboration [4] further investigated a possible negative impact on noise and laser efficiency with no visible result.

The measurements presented in this study focused on threshold current and peak wavelength shifts caused by magnetic fields. Only during one special measurement (precision scan) the laser efficiency was measured. The result is shown in section 4.2.

3 Setup

3.1 Magnet

The demand of magnetic fields up to $10\,\mathrm{T}$ made it necessary to use a superconducting magnet. The difficulty of using such a magnet is that it operates at liquid helium temperature whereas the samples and fibers should ideally remain at room temperature during insertion and measurement. Furthermore the available size for samples inside the field is typically very small.

Although the temperature inside the CMS tracker will be $-10°\mathrm{C}$ we decided to perform the test at room temperature to simplify handling and ease of comparison with other measurements.

The superconducting magnet we used is shown in fig. 4. The volume for the tested device was flooded with helium gas at a controlled temperature of $25°\mathrm{C}$. A V2A stainless steel rod, to which the samples were mounted, was inserted into a cylindrical volume of $30\,\mathrm{mm}$ diameter within the magnet.

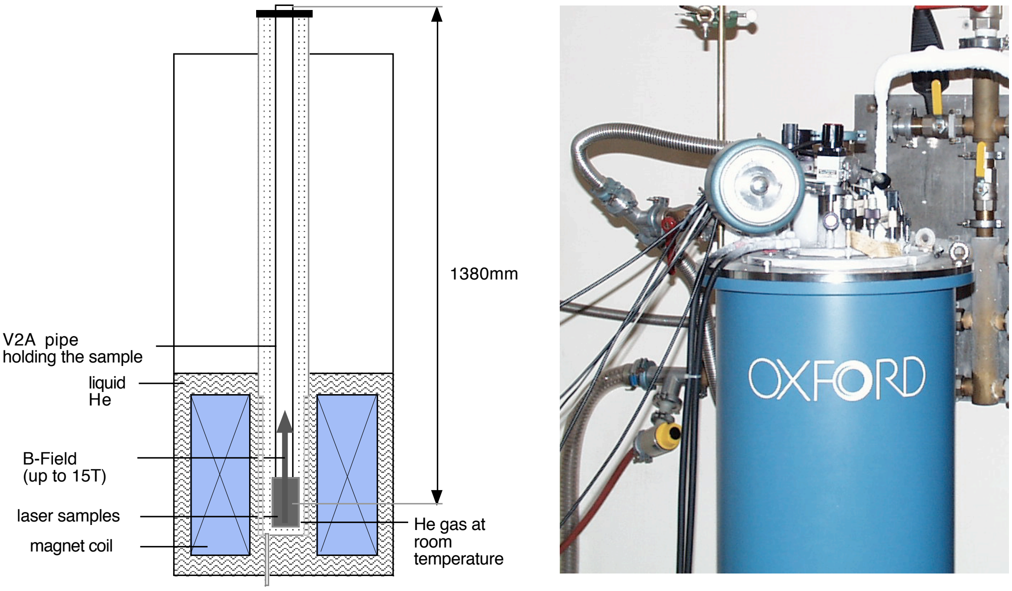

Figure 4: Schematic view and photo of the superconducting magnet.

The maximum magnetic field capability of the used magnet is $15\,\mathrm{T}$, but our tests were entirely performed in the regime of 0 up to $10\,\mathrm{T}$, where handling is much easier and liquid helium consumption is significantly reduced. Moreover, the magnetic field in the CMS tracker is only $4\,\mathrm{T}$, such that this test anyway ensures a safety margin of 250%.

3.2 Lasers under test

Lasers of two different manufacturers which were candidates for the CMS optical links were used in this test: manufacturer A (Alcatel), and manufacturer B (Italtel, now ST Microelectronics) (fig. 5). Both lasers are enclosed in a miniature package with bonding pads for the electrical connections and an undetachable single mode fiber pigtail interfacing to FC/PC connectors.

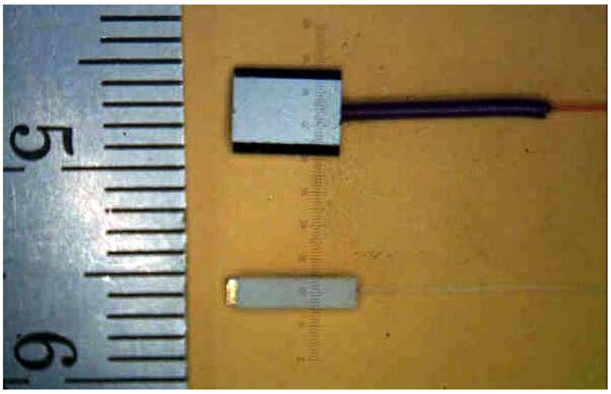

Figure 5: The two laser candidates for the CMS optical links: manufacturer B (top) and manufacturer A (bottom). The major ticks on the left scale represent centimeters.

Both types of lasers revealed a similar sensitivity to changes of temperature and magetic field strength during the tests. However, only results related to the device finally selected for use in the CMS tracker (manufacturer B, now ST Microelectronics) are presented.

3.3 Measurement setup

The two different types of lasers were tested in all three orientations, as shown in fig. 6.

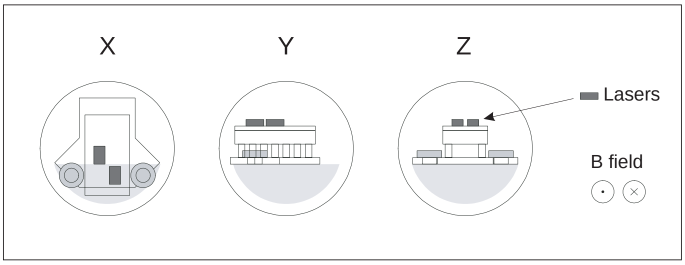

Figure 6: The three different orientations (X, Y and Z) of two semiconductor lasers on one probe with respect to the magnetic field.

The schematics of the measurement setup is illustrated in fig. 7. The lasers were driven by a programmable current source, while the light output was either connected to an optical spectrum analyzer or to a prototype of the CMS analog optical receiver to measure the output power.

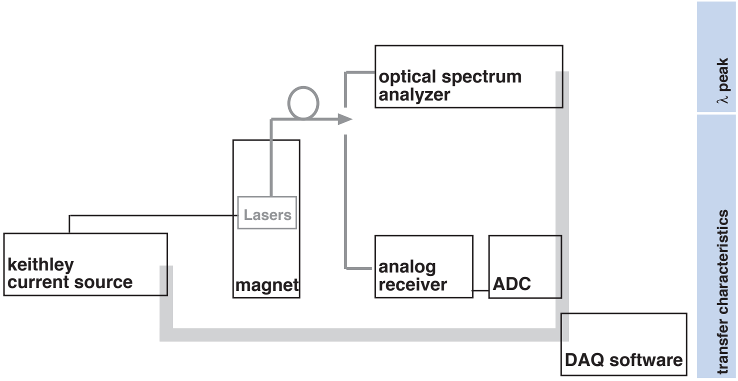

Figure 7: Setup for measurement of peak wavelength and analog performance

After installing a laser probe in a specific orientation, the magnetic field was ramped up in several steps, and two measurements were performed at each magnetic field strength. (a) The optical spectrum was measured at a bias current of $15\,\mathrm{mA}$. (b) The input/output characteristic was scanned between 0 and $20\,\mathrm{mA}$ usually and between 0 and $100\,\mathrm{mA}$ in certain cases. A final measurement at a field strength of $0\,\mathrm{T}$ was performed after the last $10\,\mathrm{T}$ measurement to be able to estimate the threshold and wavelength drifts caused by non B-field effects.

A simple peak-search was performed on each captured spectrum to evaluate the wavelength of the mode with the highest intensity λ_{peak} for each measurement (fig. 2) . To achieve a precise determination of the threshold current, a numerical differentiation of each measured analog transfer function was performed. The threshold current was then evaluated as the corresponding current to the half maximum of the resulting function. (fig. 8) This method is more robust against nonlinearities compared to intersecting linear fits.

The resulting peak wavelengths and threshold currents could then easily be compared as a function of field strength in one summarizing plot.

4 Results

4.1 Laser wavelength and threshold dependence on magnetic field

A diagram summarizing the results for two lasers of manufacturer B at one orientation is shown in fig. 9. These measurements were performed in the order $0, 4, 7, 10$ and finally $0\,\mathrm{T}$ again. It can be seen that peak wavelength and threshold current correlate for each measurement. The final measurement at $0\,\mathrm{T}$ clearly indicates that the observed

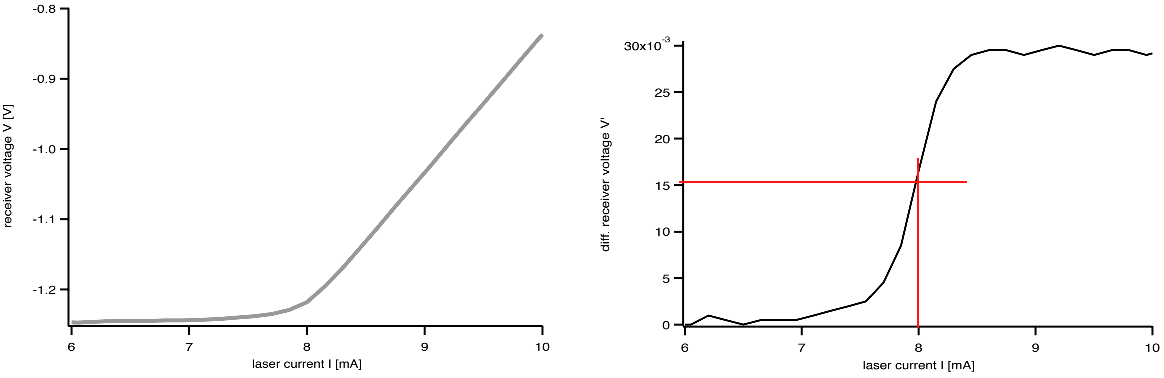

Figure 8: Evaluating the threshold current by differentiation of the transfer function

changes are most likely not dependent on the magnetic field strength but caused by thermal effects. Although the temperature of the helium gas flowing through the probe-tube had a controlled temperature, the temperature of the laser device itself was not controlled. During the experiment the devices were kept at various bias levels for an undefined amount of time. The visible changes of threshold current or peak wavelength could thus easily be attributed to self-heating of the lasers. The diagram shown is representative of all performed measurements.

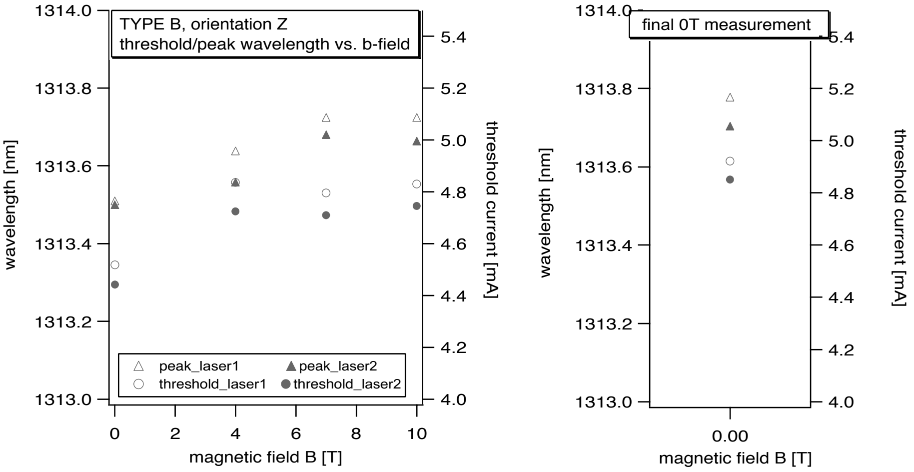

Figure 9: Result diagrams for two lasers of manufacturer B at orientation Z

4.2 Precision scan of laser threshold and efficiency dependence on magnetic field

At the end of the test, a precise scan of the magnetic field in steps of $1\,\mathrm{T}$ was performed on one laser (manufacturer B) in one orientation (X). Since only the transfer characteristics between 0 and $20\,\mathrm{mA}$ were recorded for each magnetic field strength, reconnections of the fibers could be avoided and allowed us to include an investigation of changes to the laser efficiency. The measurement of each transfer function took a very short amount of time compared to the time consumed by ramping up the magnetic field. During this time between the measurements the laser was always kept at a bias setting of $1\,\mathrm{mA}$, which minimized the influence of self-heating to the device temperature during this test.

Small shifts in the laser threshold and slope were observed when ramping up the magnetic field. As shown in fig. 10, the laser threshold decreases by about 4% at $10\,\mathrm{T}$ relative to zero field. The absolute change observed ($0.2\,\mathrm{mA}$ between $0\,\mathrm{T}$ and $10\,\mathrm{T}$) is of the same order of magnitude as the temperature effects indicated by the final

$0\,\mathrm{T}$ measurement (fig. 9) and therefore could not be observed within the accuracy of the measurements described in section 4.1.

The effect on the slope efficiency is even smaller. Fig. 11 indicates a relative increase of less than 2% at the maximum magnetic field of $10\,\mathrm{T}$.

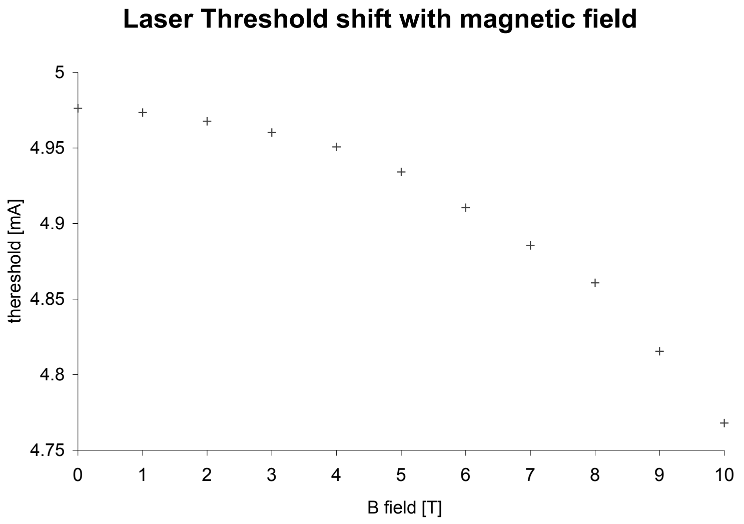

Figure 10: Laser threshold variation vs. magnetic field in the precision scan.

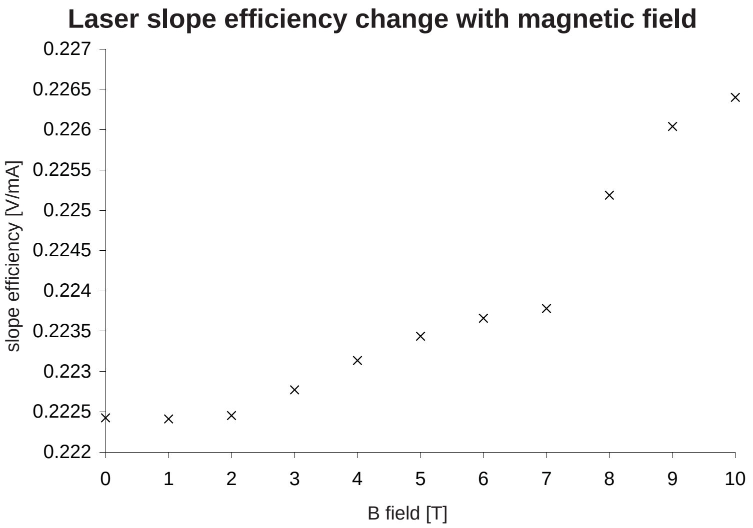

Figure 11: Laser slope efficiency variation vs. magnetic field in the precision scan.

4.3 APV25 behaviour in magnetic field

An APV25 readout chip was also tested in the magnetic field in all three orientations similar to the lasers. Noise, internal and external calibration were measured at 0, 4 and $10\,\mathrm{T}$.

The APV25 performance was completely indifferent to the presence of a magnetic field. Fig. 12 shows an overlay plot of the internal calibration waveform in deconvolution mode for the three different orientations (X, Y and Z) and magnetic fields between 0 and $10\,\mathrm{T}$. The average noise deviation between any two measurements was less than 2%, which is the usual tolerance and not related to the magnetic field.

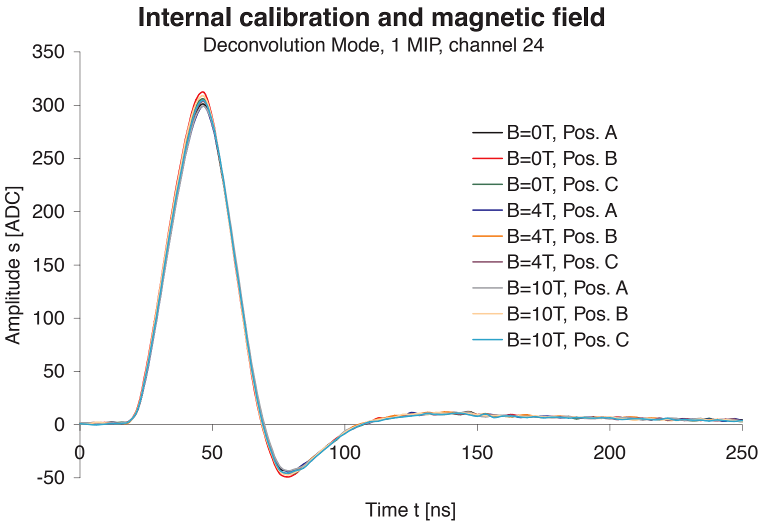

Figure 12: Overlay plot of the internal calibration waveform in deconvolution mode for the three different orientations (X, Y and Z) and magnetic fields of 0, 4 and $10\,\mathrm{T}$. Obviously the APV chip is not affected by the presence of a magnetic field.

5 Conclusions

CMS-Tracker candidate lasers of two different manufacturers were tested for threshold and spectrum shift caused by high magnetic fields up to $10\,\mathrm{T}$ in all three geometrical orientations. The measured threshold and peak wavelength shifts were dominated by temperature effects that can be attributed to laser self-heating during the measurement. In a special setup (precisionscan), the measurement accuracy was improved by minimizing the influence of laser self-heating. Small threshold and peak wavelength shifts as well as efficiency changes were observed, that were correlated to the magnetic field strength.

The results of all measurements compare well with theoretical expectations and previous tests. They clearly indicate, that the influence of magnetic fields up to $10\,\mathrm{T}$ will have a negligible impact on the analog and optical performance of the CMS-Tracker optical links.

Finally, evaluating the effects of the magnetic field on an operating APV25 readout chip showed no visible effect on its performance.

Acknowledgements

We would like to express our gratitude to Wolfgang Lang of the Institute of Material Sciences, Vienna, Austria, for providing and operating the magnet facility, and to Francois Vasey, CERN, Geneva, Switzerland, and his group for supplying the laser diodes.

References

[1] L.L.Jones et al., **The APV25 Deep Submicron Chip for CMS Detectors**, *CERN-99-09, p.162-166, September 1999* (`http://doc.cern.ch/yellowrep/1999/99-09/p162.pdf`)

[2] F.Vasey et al., **Laser based optical links for the CMS tracker: options and choices**, *CMS Note 1997/053*

[3] F.Jensen et al., **Evaluation and selection of analogue optical links for the CMS tracker - methodology and application**, *CMS Note 1999/074*

[4] F.Jensen et al., **In-system performance of MQW lasers exposed to high magnetic field**, *CMS Note 2000/040*

[5] T.Paoli, **A new technique for measuring the thermal impedance of junction lasers**, *IEEE-Journal of Quantum Electronics, Vol. QE-11 n. 7.Jul. 75*

[6] C.A.Bersbeth, **Le laser semiconducteur a cavite externe courte**, *PhD report n. 1242, EPFL, 1994*

[7] T.T.J.M. Berendschot et al., **Wavelength and threshold current of a quantum well laser in a strong magnetic field**, *Applied Physical Letters 54(19), pp. 1827-1829, 1989*

[8] T.Sato et al., **Frequency shift of a GaAlAs diode laser in a magnetic field**, *Electronic letters, Vol. 22, No. 19, pp. 979-981, 1986*

[9] T.Sato et al., **Oscillation wavelength shifts of visible and infrared laser diodes in a magnetic field"**, *Proceedings of SPIE, Vol. 3415, pp. 173-181, 1998.*

[10] J.O.Gorman et al., **Wavelength dependence of T0 in InGaAsP semiconductor laser diodes**, *Applied Physical Letters 62-2009(1993)*

[11] M.Sugawara et al., **Threshold current and its temperature dependence in InGaAsP/InP strained quantum well lasers under a magnetic field**, *Jpn. J. Appl. Phys. Vol. 34, pp. 1583-1584, 1995.*